Studying the Influence of Sea Ice Lead Fraction on Wintertime Cloud Macro- and Microphysical Properties During MOSAiC

Pablo Saavedra Garfias[1,*], Heike Kalesse-Los[1], Luisa von Albedyll[2], Hannes Griesche[3], Gunnar Spreen[4]

[1]University of Leipzig, Institute for Meteorology, Faculty of Physics and Geosciences

[2]Alfred Wegener Institute, Helmholtz Centre for Polar and Marine Research (AWI)

[3]Leipzig Institute for Tropospheric Research (TROPOS)

[4]University of Bremen, Institute of Environmental Physics

*Contact: pablo.saavedra@uni-leipzig.de

1.- Research Objectives

The study focuses on the observation of Arctic mixes-phase clouds and sea ice leads to address the following research questions:

- Are cloud properties influenced by the presence of sea ice leads?
- In which way does the coupling/decoupling of clouds to moisture-layers impact the cloud's properties?

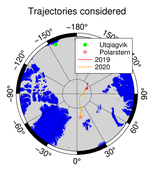

Of main interest is the wintertime/early spring legs 1 to 3 of the *MOSAiC* expedition [1] when sea ice leads occured. Instrumention and data set are mainly provided by the Atmospheric Radiation Measurement's (ARM) Mobile Facility 1 (AMF-1) and by the OCEANET-Atmosphere container from TROPOS.

The case study of 18 Nov 2019 is used to highlight the reseach methods.

2.- Coupling of Sea Ice and Clouds

Daily sea ice lead fraction (LF) is obtained from space-borne observations based on the divergence calculations from consecutive Sentinel-1 SAR scenes [4]. Additionally, sea ice concentration (SIC) is also provided by the University of Bremen [5]. Fig. 1 summarizes the LF and SIC during the period of interest.

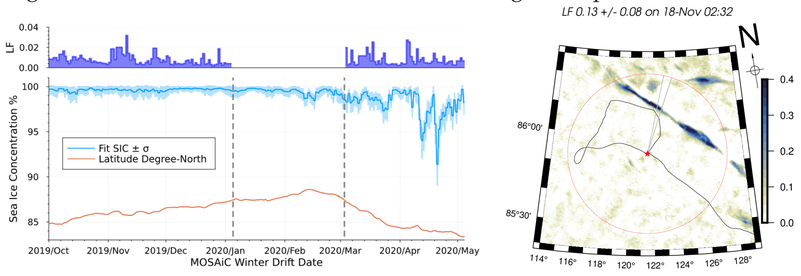

Figure 1: Left: LF and SIC for *MOSAiC* leg 1 to 3. Vertical dashed-grey lines indicates period without Sentinel-1 data. Right: case study 18 Nov 2019.

The following analysis is performed to relate sea ice lead fraction to cloud observations above RV *Polarstern* :

- LF products is analyzed for a sector 50 km around the RV *Polarstern* (red star in Fig. 1, right) with updated coordinates every minute.

- Sea ice - atmosphere coupling conceptual model

Vertical gradient of water vapour transport (∇WVT) is calculated from specific humidity q_v [g g^{-1}] and horizontal wind $\vec{v}_w$ [m s^{-1}] from radiosonde profiles, following

$$\nabla \mathrm{WVT} = -\frac{10^2}{g} \left| q_v \cdot \vec{v}_w \right| \frac{dP}{dz} \tag{1}$$

The direction of maximum transport (see grey lines in Fig. 1) is used to relate LF with zenith observations at RV *Polarstern*.

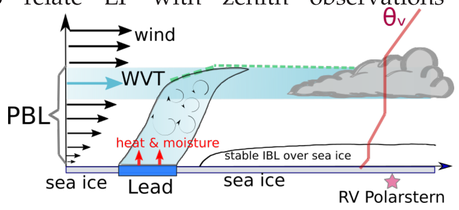

Figure 2: Sea ice interaction with observed clouds. Adapted from [7]

- Planetary boundary layer height (PBLH)

The PBLH is used as top layer from which the maximum ∇WVT is localized downwards. To have a rough estimation of PBLH, the bulk Richardson number defined as

$$Ri_b(z) = \frac{g}{\theta_v} \frac{\Delta\theta_v \, \Delta z}{(\Delta u)^2 + (\Delta v)^2} \tag{2}$$

with g is the constant of gravity, θ_v is the virtual potential temperature profile in K, $\Delta\theta_v = \theta_v - \theta_v(z_0)$, $\Delta u = u - u_0$, and $\Delta v = v - v_0$, the horizontal wind components in m s^{-1}. The $\Delta z = z - z_0$ with z the altitude of the atmosphere layers in m and the subscript 0 indicating the surface reference.

- Cloud coupling classification: criteria based on the virtual potential temperature θ_v and location of maximum ∇WVT below PBLH. The θ_v is analyzed to classify cases where the WVT is coupled or decoupled to the cloud.

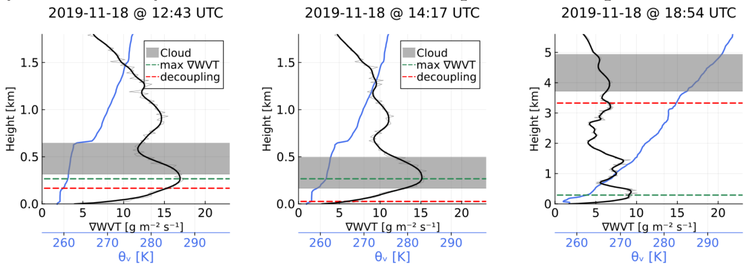

Figure 3: Examples of cloud coupling (left & middle) and decoupling (right).

3.- Results for cloud-sea ice coupled case study 18th Nov 2019

Cloudnet target classification is used to determine cloud macro- and microphysical properties. Radiosonde observations are exploited to obtain information on the thermodynamic states of the atmosphere, e.g. θ_v, ∇WVT, wind vectors, and Ri_b.

- Synergy of the ship-based zenith observations are needed to apply the Cloudnet classification algorithm.

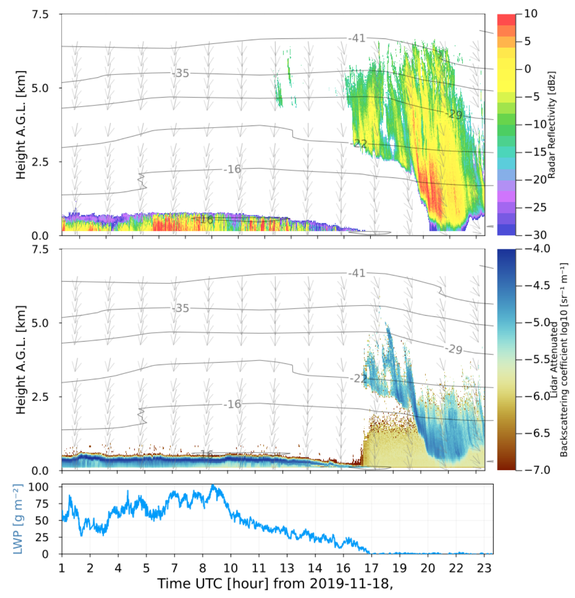

Figure 4: From top to bottom: ARM KAZR cloud radar reflectivity, ARM ceilometer backscattering coefficient, liquid water path from HATPRO microwave radiometer [2].

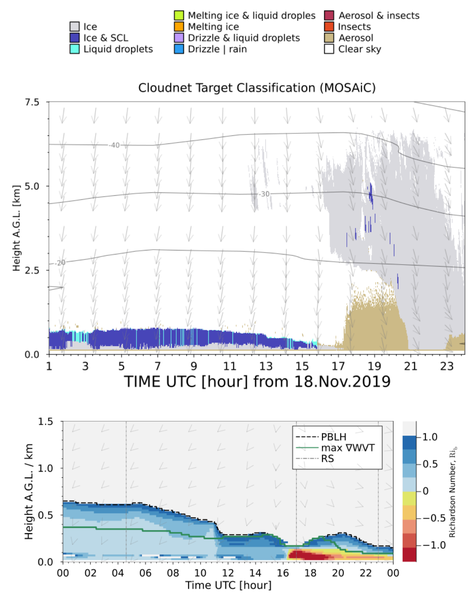

Figure 5: Top: Cloudnet classification output from the measurements in Fig. 4. Bottom: bulk Richardson number for the lowest 1.5 km, with critical Ri_b=1 as threshold for PBLH. RS denotes times of radiosonde launches.

- Cloud base and -top height (CBH and CTH, respectively) are determined only for mixed-phase clouds for up to three cloud layers from the Cloudnet target classification class (Fig. 5, top). To estimate CBH the Cloudnet pixels with liquid droplets or super-cooled liquid (SCL) are considered, for CTH the ice pixels are used in additon (Fig. 6).

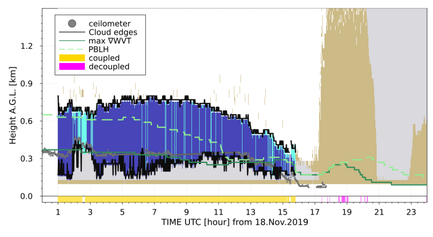

Figure 6: Close-up of Fig. 5 (top) showing the PBLH (dashed-light-green), max ∇WVT (green), and estimated cloud bottom and top heights (black lines) of the low-level stratiform mixed-phase cloud, the dotted-grey is the cloud base as detected by the ceilometer. Coupled status is shown along the x-axis.

Using Cloudnet liquid and ice water content retrievals (lwc & iwc, respectively), the total water path for liquid and ice (LWP & IWP) are calculated by integrating their water content from cloud base to cloud top for individual cloud layers (Fig. 7).

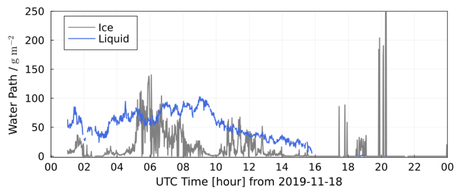

Figure 7: LWP and IWP for the lowest layer detected in Fig. 6. Note that only of mixed-phase clouds are considered.

The wind direction at max ∇WVT provides the relevant information to link sea ice LF to the cloud observation above RV *Polarstern* . LF is considered from a region determined by the wind direction with center at RV *Polarstern* to 50 km radius (grey lines in Fig. 1, right).

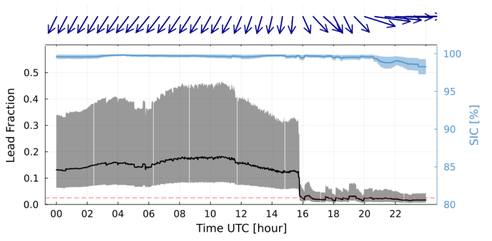

Figure 8: LF extracted from Fig. 1 (right) based on 1-minute wind direction at the max ∇WVT. For reference the wind vectors at max ∇WVT (top panel) and SIC for the same region is also shown in light-blue (right y-axis).

- From Fig. 8 the 1-minute LF statistics can be related to the corresponding micro- and macrophysical properties of clouds derived from Cloudnet. In order to reduce variability the following results are averaged in 15 minutes intervals i.e. every point represents ≈ 15 observations and bars are their variance within it.

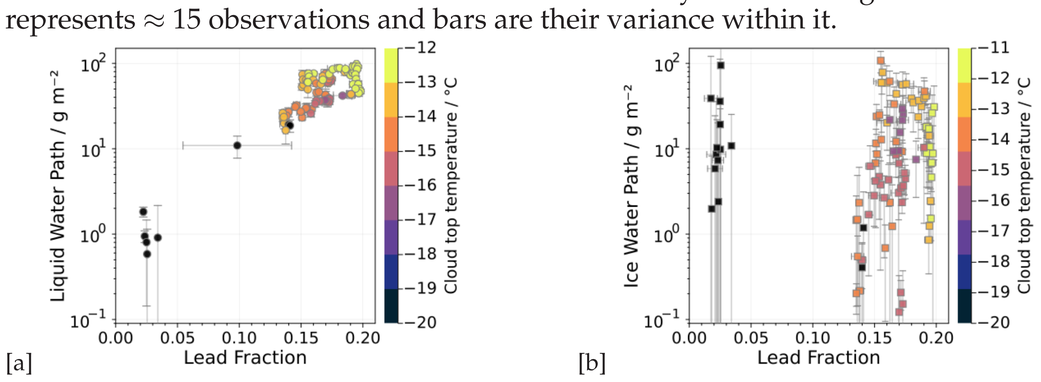

Figure 9: [a] mean single cloud layer LWP vs. LF (black-line in Fig. 8) with colour-coded cloud top temperature. [b] Same but for IWP of same cloud layer. [c] Γ_{cloud} as defined in Eq. 3 vs. LF with colour-coded cloud thickness.

From Fig. 9 [a] a clear relationship of LWP and LF can be seen, the larger the LF the higher LWP, and the warmer the cloud top temperature too. For IWP (Fig. 9 [b]) there is no relationship found, a wide range of IWP values occur during the observed LF. The only clear feature is the clustering of points with being gathered towards larger LF which corresponds to coupled cases as in Fig. 3 (left & middle).

Shown in Fig. 9 [c] is the gradient of cloud temperature defined as Eq. 3. The most negative Γ_{cloud} are close to a moist adiabatic lapse-rate, whereas positive values indicate a temperature inversion at cloud top, however this is not consistent neither with increasing LF nor cloud thickness since for coupled cases there are positive and negative Γ_{cloud} which is an indicator of other factors playing a role.

$$\Gamma_{\mathrm{cloud}} = \frac{\Delta T}{\Delta H} = \frac{T_{top} - T_{base}}{CTH - CBH} \tag{3}$$

4.- Conclusions

- Relating cloud observations with LF upwind with water vapour transport as conveying mechanism for the coupling seems to be plausible approach,
- A positive relationship of LWP and LF has been found; no clear relation between LF and IWP or cloud temperature gradient was found,
- Larger LF are acompanied by warmer cloud top, indicating a higher moisture content for those cases,
- It is confirmed that uncoupled clouds are mostly high level clouds, as also found for long-term observations at Utiqiaġvik, Alaska [6],
- SAR based LF at 700 m spatial resolution are crucial, for this case study the same results cannot be reproduce by using passive SIC retrievals at 1 km resolution (see different pattern of SIC and LF in Fig. 8,

Statistics based on this methodology are being prepared for the whole *MOSAiC* wintertime expedition in order enrich the results based on this case study.

5.- References

1. Shupe, M. et al. "Overview of the *MOSAiC* expedition Atmosphere, Elementa: Science of the Anthropocene, doi:10.1525/elementa.2021.00060, (2022).
2. Ebell, K. et al. "Temperature and humidity profiles, integrated water vapour and liquid water path derived from the HATPRO microwave radiometer onboard the Polarstern during the MOSAiC expedition", doi:10.1594/PANGAEA.941389, (2022).
3. Tukiainen, S. et al. "CloudnetPy: A Python package for processing cloud remote sensing data", JOSS, doi:10.21105/joss.02123, (2020).
4. von Albedyll, L. et al. "Linking sea ice deformation to ice thickness redistribution using high-resolution satellite and airborne observations", The Cryosphere, doi:10.5194/tc-15-2167-2021, (2021).
5. Ludwig, V., Spreen, G. et al. "Evaluation of a New Merged Sea-Ice Concentration Dataset at 1 m Resolution from Thermal Infrared and Passive Microwave Satellite Data in the Arctic", Remote Sensing, doi:10.3390/rs12193183, (2020).
6. Saavedra Garfias, P., Kalesse-Los, H. et al. "Climatology of clouds containing supercooled liquid in the Western and Central Arctic". American Geophysical Union (2021), ESSOAR. DOI10.1002/essoar.10509918.1
7. Michaelis J, Lüpkes C. "The Impact of Lead Patterns on Mean Profiles of Wind, Temperature, and Turbulent Fluxes in the Atmospheric Boundary Layer over Sea Ice". Atmosphere. (2022) https://doi.org/10.3390/atmos13010148

Acknowledgements

This work is supported by the DFG funded Transregio-project TR-172 "Arctic Amplification $(AC)^3$". Authors thank to DOE ARM program for providing *MOSAiC* data as well as the whole *MOSAiC* community. SIC product is obtained from the University of Bremen supported by Dr. G. Spreen. Cloud classification performed with open-source *Cloudnetpy* by ACTRIS and FMI.

Gedruckt im Universitätsrechenzentrum Leipzig